ARTICLE

Silica–Polymer Dual Layer-Encapsulated Quantum Dots with Remarkable Stability

Xiaoge Hu and Xiaohu Gao*

Department of Bioengineering, University of Washington, William H Foege Building N530M, Seattle, Washington 98195, United States

ABSTRACT Semiconductor quantum dots (QDs) are important fluorescent probes due to their high brightness, multiplexing capability, and photostability. However, applications in quantitative and *in vivo* imaging are hampered by their sensitivity to chemical environments and potential toxicity. Here we report a surprising finding that the combination of silica and amphiphilic polymer can stabilize CdSe/ZnS QDs in a broad range of chemical conditions including strong acidic solutions, which is unavailable for any of the current encapsulation technologies (*e.g.*, mercapto compounds, silica, and amphiphilic polymers) used alone. We further demonstrate the use of these ultrastable QDs as internal references in pH sensing applications. We expect this work will open exciting opportunities for *in vivo* and quantitative applications, and may help solve the toxicity problem of QDs.

KEYWORDS: quantum dots · imaging · nanotoxicity · silica · amphiphilic polymer · sensing

Semiconductor QDs have attracted great interest in biology and medicine in recent years because of their fascinating optical and electronic properties that are not available from conventional imaging agents.[1−4] However, a longstanding issue for chemical sensitivity and instability under different environments hampers QD application in quantitative imaging (a hallmark of modern biology) and *in vivo* diagnostics. Degradation might preclude QD probes from accurate quantitative analysis due to fluorescence fluctuation and result in potential toxicity when applied *in vivo* (currently high-quality QDs are mostly made from carcinogenic chemicals such as cadmium). Nanoparticle encapsulation technologies based on small molecule ligands,[5] silica,[6−10] and amphiphilic polymers[11−14] produce highly water-soluble and bright QDs, but none of them is capable of protecting QDs from chemical-induced degradation or surface modification.

Stability of QD fluorescence is of particular importance for quantitative imaging and analysis, when data obtained under different conditions are compared. However, often QD optical properties depend on the buffers and solvents used and fluorescence might drop drastically upon treatment with low pH solutions or bioconjugation reagents. In general, QD fluorescence is quenched in acidic solutions and enhanced in basic solutions.[15] Under complex *in vivo* conditions, the issue of chemical instability becomes an even greater concern as QD degradation (indicated by fluorescence changes) might result in release of heavy metal ions and severe toxicity. For example, Derfus *et al*. has shown that CdSe QDs capped with small-molecule mercapto compounds are deteriorated under ultraviolet illumination and release Cd^{2+} ions.[16] Under *in vivo* conditions, released Cd^{2+} ions tightly bind to large plasma proteins, such as metallothionein, and cannot be efficiently cleared out of the body. The excretion of Cd-metallothionein, primarily through urine, is extremely slow with a biologic half-life in the kidney of 38 years.[17] Quick clearance of intact QDs might provide one possible solution to this problem. Breakthrough work by Frangioni, Bawendi, and co-workers demonstrated that QDs with zwitterionic surface and hydrodynamic diameter smaller than 5.5 nm could be rapidly and efficiently eliminated *via* urinary excretion.[18] Unfortunately, rapid renal clearance is often undesirable for *in vivo* imaging and therapeutic delivery.[19] Furthermore, for targeted imaging and delivery, functionalization of QDs with targeting ligands (*e.g.*, antibodies, peptides, and aptamers) yields sizes beyond the renal clearance threshold and leads to QD uptake by the reticuloendothelial systems (RES). These trapped nanoparticles, depending on size and surface prop-

*Address correspondence to xgao@u.washington.edu.

Received for review July 18, 2010 and accepted September 17, 2010.

Published online September 23, 2010. 10.1021/nn1017044

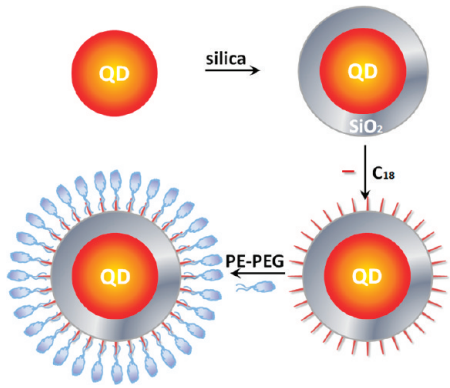

Figure 1. Schematic illustration of a double-phase transfer procedure for QD@SiO_2@PE-PEG synthesis. Single hydrophobic QDs are encapsulated within a layer of hydrophilic silica, followed by surface modification with a hydrophobic silane, OTMS. The hydrophobic QD@SiO_2−C_{18} is then solubilized with PE-PEG. Figure is not drawn to scale.

erties, could remain in animal and human bodies for long periods before final clearance. Indeed, recent investigation by Fitzpatrick *et al*. showed that systemically administered QDs persisted and retained fluorescence for up to two years in mice.[20] It was also observed that the traditional amphiphilic polymer-encapsulated QDs exhibited significant spectral blue-shift, suggesting QD degradation. This result is perhaps not surprising since QDs are not stable in acids, but their cell entry is primarily through endocytosis, a process which involves acidic cellular compartments such as late-stage endosome and lysosome. Novel surface chemistry might provide ways for accelerated *in vivo* clearance of nanomaterials. For example, near-complete secretion has been observed for carbon nanotubes coated with branched polyethyleneglycol (PEG) within two months.[21]

In this context, a key challenge is to engineer a stable coating that will maintain QD integrity and optical properties under complex chemical environments, in particular acidic solutions. This goal cannot be achieved with current capping materials based on small-molecule mercapto ligands, silica, and amphiphilic polymers. Here we report a new strategy for preparation of ultrastable QDs by combining the silica and amphiphilic polymer encapsulation techniques. To our surprise, although neither material protects QDs from harsh chemical treatments, their combination can protect QDs to such a degree that QD fluorescence remains stable even when treated with pH 1 acidic solutions. We further demonstrate the pH-sensing application of this technology by combining the ultrastable QD with a pH sensitive dye (*e.g.*, fluorescein derivative). Up to date, a handful of papers have reported the use of QDs for pH sensing based on either their pH-dependent fluctuation of absolute fluorescence intensity[22] or the FRET-based ratiometric measurements between conjugated QDs and dyes.[23,24] Despite these recent successes, a key limitation shared by virtually all current approaches is that the QD fluorescence is not only sensitive to pH but also affected by other compounds in solution. Therefore, for complex samples, it would be very difficult to distinguish the pH effect from other factors. The ultrastable QDs reported here will help solve this problem.

RESULTS AND DISCUSSION

Synthesis and characterization of ultrastable QDs. Figure 1 illustrates the major steps of the new QD encapsulation technology. The key to our success is a double phase-transfer process. Hydrophobic QDs are first encapsulated with silica shells (QD@SiO_2) based on a well-established reverse microemulsion method.[6,7,9] In contrast to prior arts where silica-coated QDs are directly used for applications, the hydrophilic QD@SiO_2 is then converted back to water-insoluble by grafting

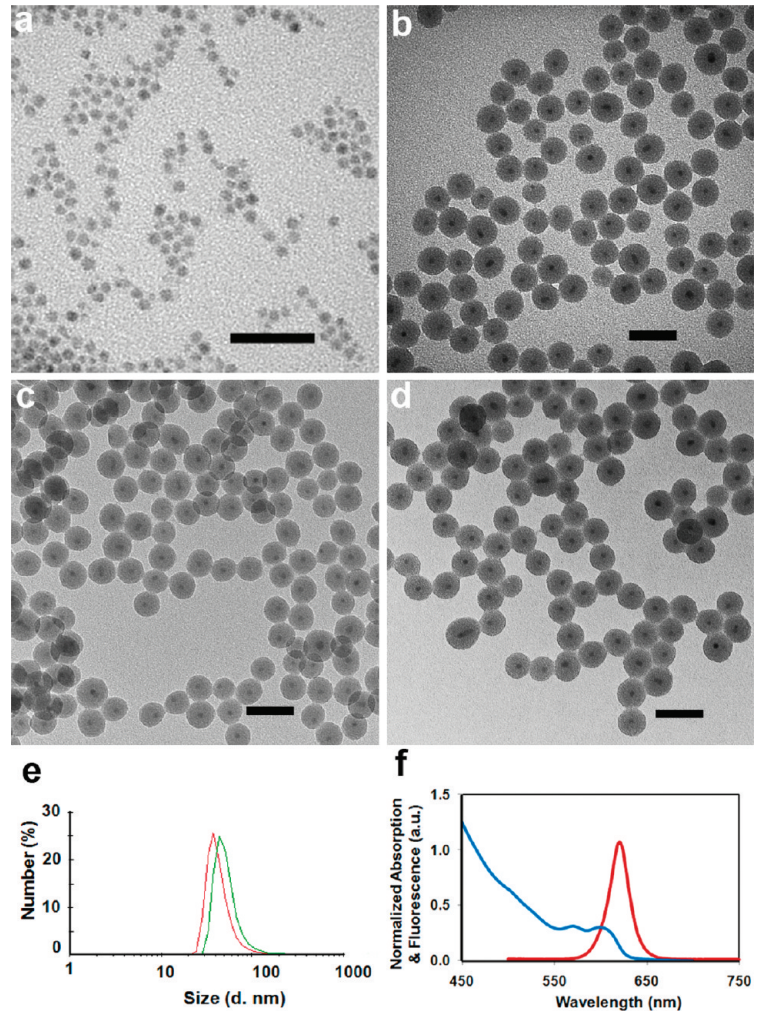

Figure 2. Characterization of QD@SiO_2@PE-PEG. TEM images of (a) CdSe/ZnS QDs dispersed in chloroform, (b) QD@SiO_2 in ethanol, (c) QD@SiO_2−C_{18} in chloroform, and (d) QD@SiO_2@PE-PEG in water. Scale bar, 50 nm. (e) DLS measurement of QD@SiO_2 and QD@SiO_2@PE-PEG showing a hydrodynamic diameter of 43.6 ± 10.6 and 53.3 ± 1.7 nm, respectively. (f) Absorbance (blue) and fluorescence (red) spectra of the QD@SiO_2@PE-PEG nanoparticles.

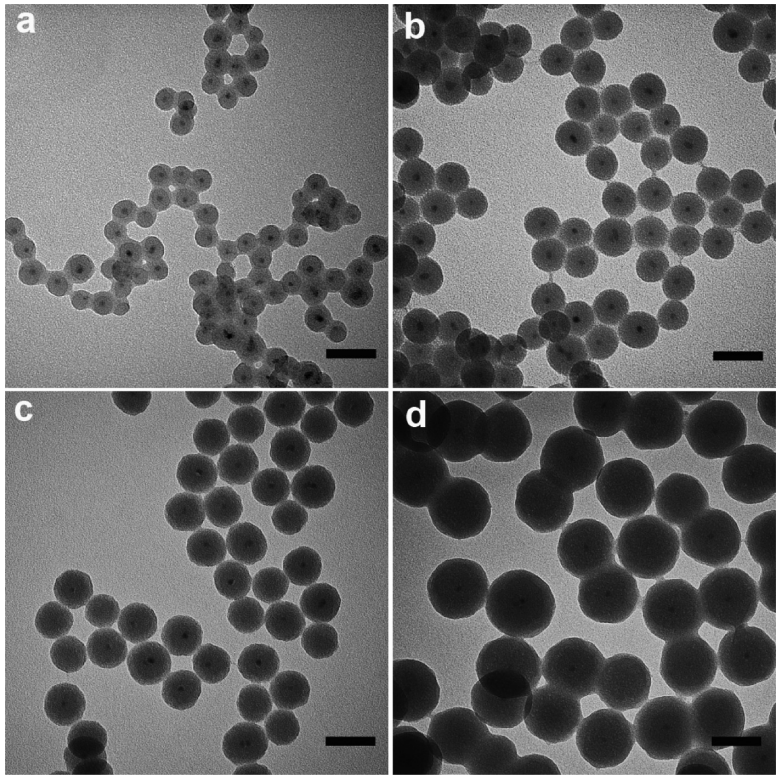

Figure 3. TEM images of QD@SiO_2 coated with silica shells of various thickness. (a) 7, (b) 13, (c) 18, and (d) 33 nm.

the silica surface with long-chain hydrocarbons (QD@SiO_2−C_{18}). Finally, the hydrophobic QD@SiO_2−C_{18} is made hydrophilic again with amphiphilic lipid-PEG molecules (QD@SiO_2@PE-PEG, complete chemical name of the amphiphilic lipid-PEG or PE-PEG is provided in the Methods section). Functional groups at the terminal of the PEG domain could enable further conjugation of targeting molecules on the surface of the nanoparticles. Note that although only PE-PEG is illustrated here, the selection of amphiphilic materials for outer surface coating is flexible. For example, amphiphilic polymers produce similar results.[11,13,14]

Figure 2a−d show representative transmission electron microscopy (TEM) images of the double-protected QD@SiO_2@PE-PEG nanoparticles compared with the original organic-soluble QDs, QD@SiO_2, and QD@SiO_2−C_{18}. All three samples of silica-coated QDs appear uniform in size and well dispersed, with the majority of the silica nanoparticles containing a single QD in the core and a few containing two QDs. The overall particle size is 32 nm and the shell thickness is 13 nm measured from the TEM images. Note that the silica shell thickness can be tuned between 5 and ~30 nm by varying the amount of TEOS precursor and QD concentration (Figure 3); nevertheless, the following discussion is based on one shell thickness, 13 nm. After further surface modification with C_{18} and PE-PEG, these layers are not visible under TEM because the organic molecules are not electron-dense materials. Apparently, the multistep modification of QDs does not cause aggregation, which is also confirmed by dynamic light scattering (DLS) measurement in an aqueous environment. The DLS results showed a hydrodynamic diameter of 43.6 ± 10.6 nm for QD@SiO_2 and 53.3 ± 1.7 nm for QD@SiO_2@PE-PEG (Figure 2e), much larger than the particle dry size. This is because the nanoparticles are pegylated and charged in solution, creating an electrical double layer surrounding the nanoparticles, and consequently increasing the colloidal hydrodynamic radius compared to the actual size.[25] Spectroscopic measurements show that the distinctive absorption and emission profiles of QDs after SiO_2 and PE-PEG coating are well preserved (Figure 2f).

Characterization of Chemical Stability. Next, we systematically compared the chemical stability of our QD@SiO_2@PE-PEG with QDs coated with traditional materials. For biological applications, QDs should be at least stable between pH 4 and 8, because (i) most bioconjugation reactions are performed in this pH range and (ii) pH values found in human body also fall in this range.[26] For example, the pH of blood is around neutral with a value of 7.4, whereas that of late-stage endosme and lysosome is about 4−5. The most basic environment can be found in the pancreas, whose secretions are of pH 8.1. In rare cases if QDs are ever going to be used for gastrointestinal (GI) tract imaging, the gastric environment has pH values around 1−2. Certainly, the exposure to gastric acid is likely to be short, before dots exit the body or are uptaken by cells. Given a wide range of potential applications, it is highly desirable to make ultrastable water-soluble QDs to minimize fluorescence fluctuation and toxicity caused by Cd^{2+} release.

Indeed, the significance of making stable QDs, with a particular focus on stability in acids (major reason for QD etching and Cd^{2+} release), is also recognized by other researchers. Recent works by Mattoussi, Nie, and co-workers suggested that QDs coated with thiolated PEG[27] and polyethylene imine (PEI)[28,29] are more acid resistant than with small-molecule mercapto compounds or amphiphilic polymers. We have confirmed the stability improvement with these coatings. However, detailed quantitative spectroscopic measurements revealed that QD fluorescence quenching at low pH was still significant (>99% at pH 1), similar to the traditional mercaptoacetic acid (MAA), silica, PE-PEG, and PMAT (poly(maleic anhydride alt-1-tetradecene)) coated QDs (Figure 4). In contrast, the fluorescence of our QD@SiO_2@PE-PEG remained constant from pH 2 to 8, and changed less than 10% at pH 1 and 9 after 1-h incubation (normalized by fluorescence at pH 7). Although higher pH values are not generally encountered in biological experiments, we still extended the stability test to a full spectrum of pH

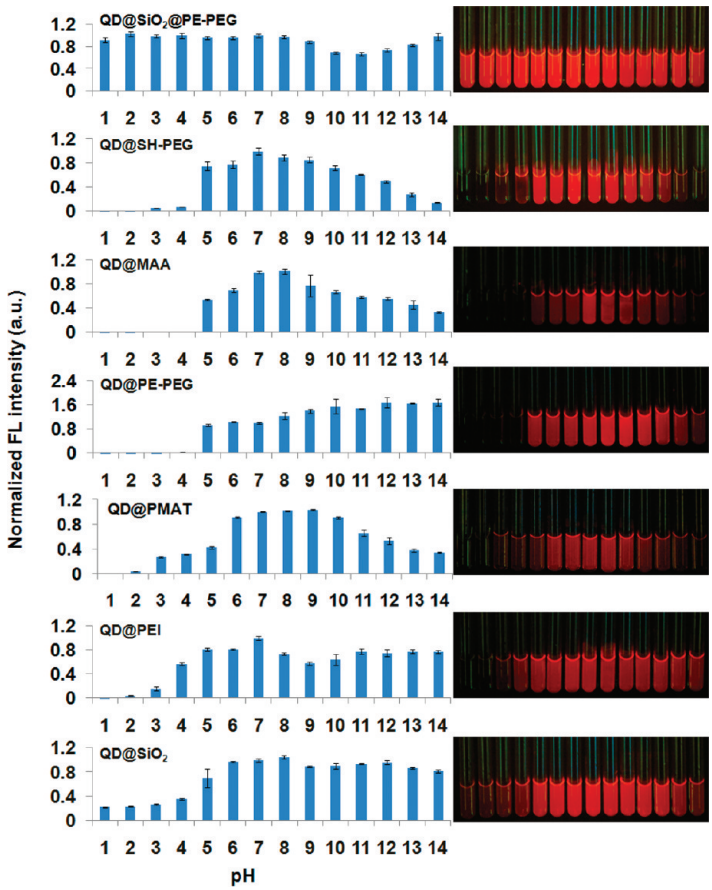

Figure 4. pH stability comparison of QD@SiO_2@PE-PEG with QDs with traditional surface coatings, QD@SH−PEG, QD@MAA, QD@PE-PEG, QD@PMAT, QD@PEI, and QD@SiO_2. The panels on the right show the corresponding fluorescence images of QDs dispersed in pH 1 to 14 solutions (illuminated with a 365 nm hand-held UV lamp).

(1−14). A decrease in fluorescence intensity was observed at pH 10 and 11, likely due to instability of silica in basic solutions, and gradually increased under more basic conditions. Such increase in QD fluorescence might be associated with partial degradation of the silica shell in strong bases followed by regained QD sensitivity to environment.

As a fluorescent labeling reagent, QDs are often subject to bioconjugation involving biomolecules and chemical cross-linkers, and thus it is important for QDs to maintain their fluorescence in the presence of common bioconjugation reagents. Compared with the traditional surface capping methods, the new QD@SiO_2@PE-PEG exhibited remarkable stability. Figure 5 shows that only the fluorescence of QD@SiO_2@PE-PEG remains constant under different chemical treatments, whereas other QD specimens exhibit deterioration in optical properties. This chemical stability could have important applications in quantitative cellular and molecular imaging.

The mechanism of this high-level protection by the silica-amphiphilic polymer coating is not entirely understood at this time. When silica or PE-PEG is used alone, neither material protects QDs from acid- or chemical-induced quenching and etching, but, when combined, the coating layer becomes significantly less permeable to water-soluble chemicals. It is known that silica shells prepared with the Stöber chemistry or its derivatives have a porosity of 10−15% with pores on the order of a couple of nanometers,[30] allowing ions to diffuse through. In the double phase-transfer process reported here, the silica shells are first modified with hydrocarbons, which likely to react not only onto the outer surface of the silica shell but also onto the pore walls (in a similar way to preparation of reverse phase chromatography resins), thus inhibiting diffusion of water-soluble compounds through the shell. This and other possible mechanisms deserve further systematic studies. Nevertheless, following solubilization with the amphiphilic PE-PEG molecules, QDs became both colloidally and chemically stable. The combination of the silica encapsulation and the hydrophobic double layer provides a robust, inert shell layer against nanoparticle degradation. The presence of PEG chains not only imparts the water solubility of particles, but also flexible bioconjugation since COOH-, NH_2-, and OH-terminated PEG are widely available.

Cytotoxicity. As one of the major potential applications for ultrastable QDs is *in vivo* imaging and drug delivery, we further probed the cytotoxicity of QD@SiO_2@PE-PEG in LNCaP cells. Please note

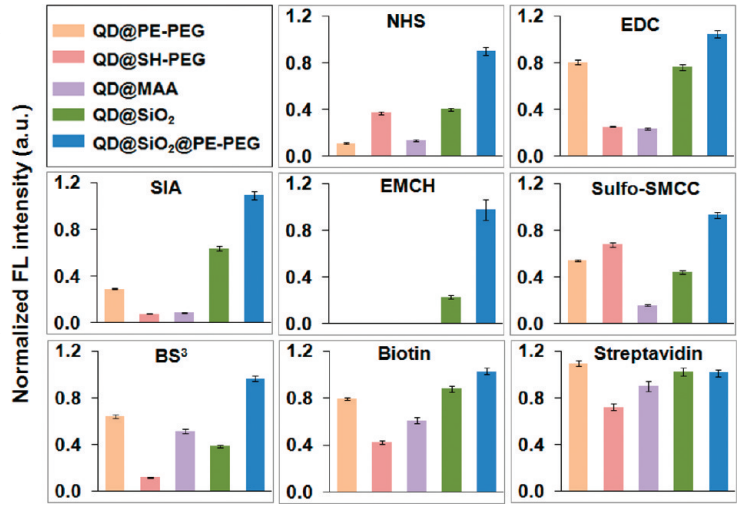

Figure 5. Stability comparison of the various QDs treated with common cross-linking reagents in bioconjugation, 5 mM EDC, NHS, SIA, EMCH, 0.25 mM sulfo-SMCC and BS^3, 0.05 mg/mL biotin and streptavidin. The color codes of the samples are shown in the first panel.

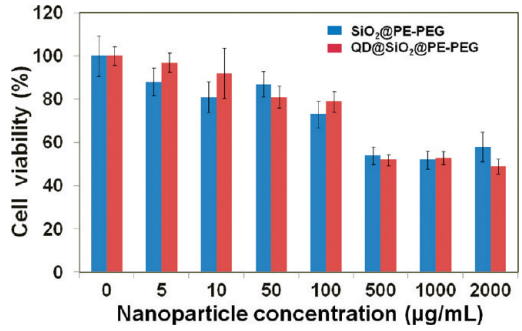

Figure 6. Cytotoxicity evaluation of QD@SiO_2@PE-PEG compared with SiO_2@PE-PEG (no QD doping). Dose-dependent viability evaluation of LNCaP cells treated with QD@SiO_2@PE-PEG (red) and SiO_2@PE-PEG (blue) of the same size. The toxicities of the two samples exhibit nearly identical trend of dose-dependent behavior, indicating that the toxicity is due to the colloidal particles, but not the QDs doped inside.

that the LNCaP cells merely serve as a model. Additional cell types derived from multiple target tissues will be needed for more stringent toxicity tests. Below 100 μg/mL (approximately 6 nM measured with UV absorption at first extinction peak of the QDs), cell viability after incubation with QD@SiO_2@PE-PEG for 24 h is above 80%. This is in the typical concentration range for cellular staining with QD bioconjugates or QDs diluted in blood circulation under *in vivo* conditions.[1−4] At elevated concentrations (*e.g.*, 500−2000 μg/mL), cell viability decreases to approximately 60% after 24-h incubation. Nevertheless, compared with plain silica nanoparticles (no QDs inside) of similar sizes and surface coating (SiO_2@PE-PEG) (Supporting Information, Figure S1), the concentration-dependent toxicity of QD@SiO_2@PE-PEG shows virtually an identical trend to that of SiO_2@PE-PEG (Figure 6), suggesting that the observed toxicity is only due to the presence of colloidal nanoparticles in solution but not QD degradation and Cd^{2+} release, which also confirms the stability of QD@SiO_2@PE-PEG in biological systems.

pH Sensing. Based on this new series of ultrastable QDs, we show that they can be used for pH sensing applications and serve as an internal reference. Previously a number of groups have built QD-based pH sensors because QDs are sensitive to chemicals in the surrounding environment such as acids, bases, ions, and proteins. For example, pH values can be directly correlated with QD fluorescence intensity because QD fluorescence, in general, is quenched in acids and is enhanced in bases.[22] However, this direct measurement is limited to conditions when the total QD quantity is fixed. Under dynamic conditions such as QD endocytosis and exocytosis, it would be very difficult to correlate pH values with absolute QD fluorescence. A more elegant and robust approach is to use ratiometric measurements such as by using QD-dye FRET (fluorescence resonance energy transfer) pairs, because fluorescence intensity ratios are irrespective of changes in probe quantity, excitation intensity, and detector sensitivity.[23,24] However, as aforementioned, QD fluorescence fluctuation is not specific to pH values (or concentrations of H^+ and OH^-). The presence of other ions or molecules could also change the fluorescence intensity ratios and consequently lead to misinterpretation of experimental results. Here, we design a novel ratiometric pH sensor where ultrastable QDs are only used as internal references. A pH-sensitive fluorophore, 4′-aminomethyl fluorescein, hydrochloride (AMF), is immobilized to the surface of QD@SiO_2@PE-PEG *via* an amide bond. In such a configuration, FRET between the dye and QD should have minimal effect on the ratiometric measurement because of the large separation between the core QDs and surface attached dye molecules and the efficient excitation of QDs (due to the QDs' broad absorption profile) regardless of energy donation from dye molecules. As shown in Figure 7a, AMF fluorescence has a sharp transition between pH values 4−9, which serve

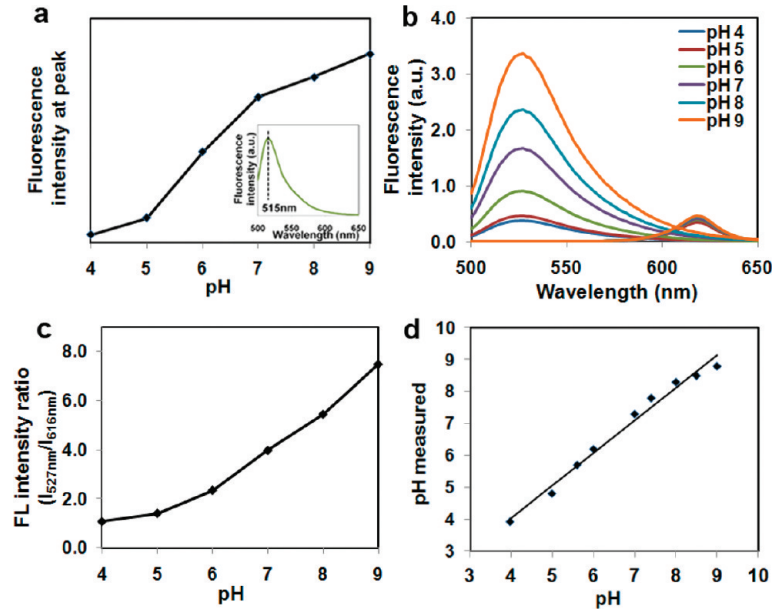

Figure 7. pH sensing using QD-AMF dual-color sensor: (a) pH-dependent emission of AMF fluorescence measured at the peak (inset, a representative AMF spectrum); (b) fluorescence emission of QD-AMF conjugates at various pH values. The contributions from QD and AMF are separated from the composite emission spectra for accurate measurement of the peak intensities. While QD fluorescence remains constant, fluorescence from AMF fluctuates with pH. (c) Working curve for pH measurement produced with AMF/QD fluorescence intensity ratios (I_{527}/I_{616}) *versus* pH values. (d) Correlation of known pH values and those measured with the QD-AMF pH sensor using the working curve in panel c.

as the dynamic working range. The overall fluorescence of QD-AMF conjugates can be readily fitted using a linear combination of AMF and QD based on previously published procedures[31] (Figure 7b). The working curve is plotted using the fluorescence intensity ratios of AMF/QD and corresponding pH values (Figure 7c). When a separate set of solutions of different pH are measured using this working curve, nearly perfect correlation (Figure 7d) is observed for the measured values using the QD-AMF sensor and the real values (buffers of known values and confirmed with pH papers).

CONCLUSION

We have developed a new method for preparation of ultrastable QDs by combining two current encapsulation technologies based on silica shells and amphiphilic polymers. Surprisingly, this synergistic combination yields QDs with significantly improved resistance to harsh chemical treatment including strong acids, which has never been achieved previously using either coating material alone. We further demonstrated applications of the ultrastable QDs for pH sensing. In contrast to previous reports, the QDs used here are insensitive to environment changes and only serve as an internal reference. This feature could open new opportunities in sensing applications in complex biological fluids when H^+ and OH^- are not the only solutes. We also note that the current work is mainly focused on technology development and characterization of nanoparticle properties. Applications of this new class of QDs in quantitative imaging, their *in vivo* behaviors, and long-term toxicity are currently under investigation.

MATERIALS AND METHODS

Chemicals and Instruments. Unless specified, chemicals were purchased from Sigma-Aldrich (St. Louis, MO) and used without further purification. 1-Ethyl-3-[3-dimethylaminopropyl]carbodiimide hydrochloride (EDC), N-Hydroxysuccinimide (NHS) bis[sulfosuccinimidyl] suberate (BS^3), *N*-succinimidyl iodoacetate (SIA), [*N*-*e*-maleimidocaproic acid] hydrazide, trifluoroacetic acid salt (EMCH), *N*-hydroxysulfosuccinimide esters of biotin (sulfo-NHS-biotin), and (Sulfosuccinimidyl 4-[N-maleimidomethyl]-cyclohexane-l-carboxylate)(Sulfo-SMCC) were purchased from Thermo Scientific (Rockford, IL). Streptavidin and 4′-(aminomethyl)fluorescein, hydrochloride) was obtained from Invitrogen (Carlsbad, CA). (1,2-Distearoyl-*sn*-glycero-3-phosphoethanolamine-*N*-[carboxy(polyethylene glycol)-2000] (PE-PEG) was purchased from Avanti Polar Lipids. TOPO-coated CdSe/ZnS core/shell QDs were provided by Oceannanotech, LLC as a gift. All chemicals were used as received. A Fluoromax4 fluorometer (Horiba Jobin Yvon, Edison, NJ) was used to characterize the emission spectra of QDs. TEM images were obtained on a CM100 transmission electron microscope (Philips EO, Netherlands). True-color fluorescence images were obtained with a Nikon digital camera.

Synthesis of Silica-Coated QDs. CdSe/ZnS QDs were incorporated in silica spheres by a reverse microemulsion method described by Nann *et al.*[7] Briefly, 1.3 mL of IGEPAL CO-520 was added to 10 mL of cyclohexane, followed by the addition of 2 nmol of QDs (in 100 μL chloroform), 80 μL TEOS, and 150 μL ammonia aqueous solution (30%). Between each chemical addition, the reaction mixture was stirred for 15 min. The final mixture solution was stirred continuously for 24 h in dark. After the silica condensation reaction, the QD@SiO_2 nanoparticles were isolated from the microemulsion by the addition of ethanol (3 mL) followed by centrifugation at 4000 rpm for 10 min. The resulting QD@SiO_2 nanoparticles were repeatedly rinsed with ethanol and aged for a week.

Hydrophobic Modification of QD@SiO_2. The QD@SiO_2 ethanol solution (10 mL) was mixed with 0.1 mL of ammonia solution (30%) to adjust the pH to 9. Trimethoxy(octadecyl)silane (OTMS) chloroform solution (10%, 1 mL) was added dropwise into the nanoparticle suspension under vigorous stirring. After 24 h, the particles were separated with centrifugation, washed with ethanol, and dispersed in chloroform.

Solubilization of the Hydrophobic QD@SiO_2. OTMS-coated QD@SiO_2 nanoparticles were dispersed in chloroform. PE-PEG was added in a molar ratio of 2000:1 to QD@SiO_2. The mixture was vortexed and sonicated for 5 min. Chloroform was slowly evaporated under vacuum, and the remaining nanoparticle film was dispersed in H_2O with sonication. The solution was centrifuged for 30 min at 15000 rpm to remove empty micelles (repeated three times). The resulting QD@SiO_2@PE-PEG was readily resuspended into H_2O.

Synthesis of SiO_2 Nanoparticles without QDs. Pure SiO_2 nanoparticles of similar size to QD@SiO_2 were made according to the same procedure without adding the QDs into the reverse emulsion, and the mixture was stirred for 72 h. The SiO_2 nanoparticles were treated in the same way as the QD@SiO_2 nanoparticles.

Chemical Stability Tests. For stability against acids and bases, pH values of QD solutions were tuned with HCl or NaOH, and QDs were incubated for 1 h with continuous shaking. Fluorescence of the QD samples was recorded on a Fluoromax4 fluorometer. For stability against common bioconjugation cross-linkers, QDs were probed with 5 mM EDC, 5 mM NHS, 5 mM SIA, and 5 mM EMCH, 0.25 mM sulfo-SMCC, 0.25 mM BS^3, 0.2 mM biotin, and 50 μg/mL streptavidin. The concentrations were selected according to the solubility of the chemicals in water and typical values used in bioconjugation. The corresponding fluorescence intensities were recorded after 1 h incubation.

Toxicity Comparison between QD@SiO_2 and SiO_2. LNCaP cells were cultured in RPMI-1640 medium, supplemented with 10% fetal bovine serum (FBS) and antibiotics (100 μg/mL streptomycin and 100 U/mL penicillin in a humidified atmosphere at 37 °C with 5% CO_2. CellTiter 96 Non-Radioactive Cell Proliferation assay (MTT) (Promega, San Luis Obispo, CA) was used to probe the toxicity effects of SiO_2@PE-PEG and QD@SiO_2@PE-PEG nanoparticles in living cells. At day 1, 5.0×10^3 cells were seeded in each well with 100 μL of RPMI-1640 and cultured for 24 h. On the second day, 20 μL of nanoparticles in deionized water (>18 MΩ cm^{-1}) was added to the cells. The final concentrations of nanoparticles ranged from 5 μg/mL to 2000 μg/mL. The negative control cells were treated with 20 μL of water only. After 24-h incubation, 15 μL of the dye solution in the toxicity kit was added to each well and incubated for 4 h. After incubation, 100 μL of the solubilization solution/stop mix was added to each well. The plate was allowed to stand overnight in a sealed container with a humidified atmosphere at room temperature to completely solubilize the formazan crystals. The absorbance was recorded at 570 nm wavelength using a 96-well plate reader. The percentage of survival cells was calculated as a percentage from the viability of the control cells, compared to the negative control cells. The viability of the control cells was considered 100%.

Preparation of QD−AMF Conjugate. AMF (2 mg) was dissolved to 2 mL of DMF. To 1 mL of QD@SiO_2@PE-PEG solution (0.55 μM in water), 100 μL of EDC solution (10 mg/mL) and AMF stock solution (volume varies depending on AMF/QD ratio) were added under stirring, and the reaction was kept overnight. The resulting QD−AMF conjugates were purified by repeated centrifugal filtering (Millipore, 50 kDa MWCO) to remove excess dyes.

Acknowledgment. This work was supported in part by NIH (R01CA131797, R01ES016189), NSF (0645080), and the UW Department of Bioengineering. X.H.G. thanks the NSF for a Faculty Early Career Development award (CAREER). We thank P. Zrazhevskiy for assistance with QD toxicity experiments and critical reading of the paper, and F. Zhang on discussion of QD pH sensors. We are also grateful to Profs. T.J. Kavanagh and D. Eaton for fruitful discussion on nanotoxicity, and Dr. Y. A. Wang at Oceannanotech for high-quality QDs.

Supporting Information Available: TEM images of the QD@SiO_2@PE-PEG and SiO_2@PE-PEG used in the toxicity study. This material is available free of charge *via* the Internet at http://pubs.acs.org.

REFERENCES AND NOTES

1. Medintz, I. L.; Uyeda, H. T.; Goldman, E. R.; Mattoussi, H. Quantum Dot Bioconjugates for Imaging, Labelling and Sensing. *Nat. Mater.* **2005**, *4*, 435–446.
2. Michalet, X.; Pinaud, F. F.; Bentolila, L. A.; Tsay, J. M.; Doose, S.; Li, J. J.; Sundaresan, G.; Wu, A. M.; Gambhir, S. S.; Weiss, S. Quantum Dots for Live Cells. In Vivo Imaging, and Diagnostics. *Science* **2005**, *307*, 538–544.
3. Zrazhevskiy, P. ; Sena, M. ; Gao, X. , Designing Multifunctional Quantum Dots for Bioimaging, Detection, and Drug Delivery. Chem. Soc. Rev., published online August 9, 2010, http://dx.doi.org/10.1039/B915139G.
4. Zrazhevskiy, P.; Gao, X. Multifunctional Quantum Dots for Personalized Medicine. *Nano Today* **2009**, *4*, 414–428.
5. Chan, W. C. W.; Nie, S. M. Quantum Dot Bioconjugates for Ultrasensitive Nonisotopic Detection. *Science* **1998**, *281*, 2016–2018.
6. Selvan, S. T.; Tan, T. T.; Ying, J. Y. Robust, Non-Cytotoxic, Silica-Coated CdSe Quantum Dots with Efficient Photoluminescence. *Adv. Mater.* **2005**, *17*, 1620–1625.
7. Darbandi, M.; Thomann, R.; Nann, T. Single Quantum Dots in Silica Spheres by Microemulsion Synthesis. *Chem. Mater.* **2005**, *17*, 5720–5725.
8. Bruchez, M.; Moronne, M.; Gin, P.; Weiss, S.; Alivisatos, A. P. Semiconductor Nanocrystals as Fluorescent Biological Labels. *Science* **1998**, *281*, 2013–2016.
9. Koole, R.; van Schooneveld, M. M.; Hilhorst, J.; Donega, C. D.; 't Hart, D. C.; van Blaaderen, A.; Vanmaekelbergh, D.; Meijerink, A. On The Incorporation Mechanism of Hydrophobic Quantum Dots in Silica Spheres by A Reverse Microemulsion Method. *Chem. Mater.* **2008**, *20*, 2503–2512.
10. Zhang, T.; Stilwell, J. L.; Gerion, D.; Ding, L.; Elboudwarej, O.; Cooke, P. A.; Gray, J. W.; Alivisatos, A. P.; Chen, F. F. Cellular Effect of High Doses of Silica-Coated Quantum Dot Profiled with High Throughput Gene Expression Analysis and High Content Cellomics Measurements. *Nano Lett.* **2006**, *6*, 800–808.
11. Pellegrino, T.; Manna, L.; Kudera, S.; Liedl, T.; Koktysh, D.; Rogach, A. L.; Keller, S.; Rädler, J.; Natile, G.; Parak, W. J. Hydrophobic Nanocrystals Coated with an Amphiphilic Polymer Shell: A General Route to Water Soluble Nanocrystals. *Nano Lett.* **2004**, *4*, 703–707.
12. Dubertret, B.; Skourides, P.; Norris, D. J.; Noireaux, V.; Brivanlou, A. H.; Libchaber, A. *In Vivo* Imaging of Quantum Dots Encapsulated in Phospholipid Micelles. *Science* **2002**, *298*, 1759–1762.
13. Gao, X. H.; Cui, Y. Y.; Levenson, R. M.; Chung, L. W. K.; Nie, S. M. *In Vivo* Cancer Targeting and Imaging with Semiconductor Quantum Dots. *Nat. Biotechnol.* **2004**, *22*, 969–976.
14. Wu, X. Y.; Liu, H. J.; Liu, J. Q.; Haley, K. N.; Treadway, J. A.; Larson, J. P.; Ge, N. F.; Peale, F.; Bruchez, M. P. Immunofluorescent Labeling of Cancer Marker Her2 and Other Cellular Targets with Semiconductor Quantum Dots. *Nat. Biotechnol.* **2003**, *21*, 41–46.
15. Spanhel, L.; Haase, M.; Weller, H.; Henglein, A. Photochemistry of Colloidal Semiconductors. 2. Surface Modification and Stability of Strong Luminescing CdS Particles. *J. Am. Chem. Soc.* **1987**, *109*, 5649–5655.
16. Derfus, A. M.; Chan, W. C. W.; Bhatia, S. N. Probing The Cytotoxicity of Semiconductor Quantum Dots. *Nano Lett.* **2004**, *4*, 11–18.
17. Goyer, R. A. Toxic and Essential Metal Interactions. *Annu. Rev. Nutr.* **1997**, *17*, 37–50.
18. Soo Choi, H.; Liu, W.; Misra, P.; Tanaka, E.; Zimmer, J. P.; Itty Ipe, B.; Bawendi, M. G.; Frangioni, J. V. Renal Clearance of Quantum Dots. *Nat. Biotechnol.* **2007**, *25*, 1165–1170.
19. Weissleder, R.; Bogdanov, A.; Neuwelt, E. A.; Papisov, M. Long-Circulating Iron-Oxides for MR-Imaging. *Adv. Drug Delivery Rev.* **1995**, *16*, 321–334.
20. Fitzpatrick, J. A. J.; Andreko, S. K.; Ernst, L. A.; Waggoner, A. S.; Ballou, B.; Bruchez, M. P. Long-Term Persistence and Spectral Blue Shifting of Quantum Dots *in Vivo*. *Nano Lett.* **2009**, *9*, 2736–2741.
21. Liu, Z.; Davis, C.; Cai, W.; He, L.; Chen, X.; Dai, H. Circulation and Long-Term Fate of Functionalized, Biocompatible Single-Walled Carbon Nanotubes in Mice Probed by Raman Spectroscopy. *Proc. Natl. Acad. Sci. U.S.A.* **2008**, *105*, 1410–1415.
22. Liu, Y. S.; Sun, Y. H.; Vernier, P. T.; Liang, C. H.; Chong, S. Y. C.; Gundersen, M. A. pH-Sensitive Photoluminescence of CdSe/ZnSe/ZnS Quantum Dots in Human Ovarian Cancer Cells. *J. Phys. Chem. C* **2007**, *111*, 2872–2878.
23. Jin, T.; Sasaki, A.; Kinjo, M.; Miyazaki, J. A Quantum Dot-Based Ratiometric pH Sensor. *Chem. Commun.* **2010**, *46*, 2408–2410.
24. Snee, P. T.; Somers, R. C.; Nair, G.; Zimmer, J. P.; Bawendi, M. G.; Nocera, D. G. A Ratiometric Cdse/Zns Nanocrystal pH Sensor. *J. Am. Chem. Soc.* **2006**, *128*, 13320–13321.
25. Shenhar, R.; Norsten, T. B.; Rotello, V. M. Polymer-Mediated Nanoparticle Assembly: Structural Control and Applications. *Adv. Mater.* **2005**, *17*, 657–669.
26. Boron, W. F.; Boulpaep, E. L. *Medical Physiology: A Cellular and Molecular Approach;* Elsevier/Saunders: Philadelphia, PA, 2004.
27. Mei, B. C.; Susumu, K.; Medintz, I. L.; Mattoussi, H. Polyethylene Glycol-Based Bidentate Ligands To Enhance Quantum Dot and Gold Nanoparticle Stability in Biological Media. *Nat. Protoc.* **2009**, *4*, 412–423.
28. Duan, H. W.; Nie, S. M. Cell-Penetrating Quantum Dots Based on Multivalent and Endosome-Disrupting Surface Coatings. *J. Am. Chem. Soc.* **2007**, *129*, 3333–3338.
29. Mohs, A.; Duan, H.; Kairdolf, B.; Smith, A.; Nie, S. Proton-Resistant Quantum Dots: Stability in Gastrointestinal Fluids and Implications for Oral Delivery of Nanoparticle Agents. *Nano Res.* **2009**, *2*, 500–508.
30. Szekeres, M.; Toth, J.; Dekany, I. Specific Surface Area of Stoeber Silica Determined by Various Experimental Methods. *Langmuir* **2002**, *18*, 2678–2685.
31. Goldman, E. R.; Clapp, A. R.; Anderson, G. P.; Uyeda, H. T.; Mauro, J. M.; Medintz, I. L.; Mattoussi, H. Multiplexed Toxin Analysis Using Four Colors of Quantum Dot Fluororeagents. *Anal. Chem.* **2003**, *76*, 684–688.